The parietal reach region is limb specific and not involved in eye-hand coordination

Eric A. Yttri, Cunguo Wang, Yuqing Liu and Lawrence H. Snyder

J Neurophysiol 111:520-532, 2014. First published 6 November 2013; doi:10.1152/jn.00058.2013

J Neurophysiol 111: 520–532, 2014.
First published November 6, 2013; doi:10.1152/jn.00058.2013.

The parietal reach region is limb specific and not involved in eye-hand coordination

Eric A. Yttri, Cunguo Wang, Yuqing Liu, and Lawrence H. Snyder
Department of Anatomy and Neurobiology, Washington University School of Medicine, St. Louis, Missouri

Submitted 24 January 2013; accepted in final form 5 November 2013

Yttri EA, Wang C, Liu Y, Snyder LH. The parietal reach region is limb specific and not involved in eye-hand coordination. *J Neurophysiol* 111: 520–532, 2014. First published November 6, 2013; doi:10.1152/jn.00058.2013.—Primates frequently reach toward visual targets. Neurons in early visual areas respond to stimuli in the contralateral visual hemifield and without regard to which limb will be used to reach toward that target. In contrast, neurons in motor areas typically respond when reaches are performed using the contralateral limb and with minimal regard to the visuospatial location of the target. The parietal reach region (PRR) is located early in the visuomotor processing hierarchy. PRR neurons are significantly modulated when targets for either limb or eye movement appear, similar to early sensory areas; however, they respond to targets in either visual field, similar to motor areas. The activity could reflect the subject's attentional locus, movement of a specific effector, or a related function, such as coordinating eye-arm movements. To examine the role of PRR in the visuomotor pathway, we reversibly inactivated PRR. Inactivation effects were specific to contralateral limb movements, leaving ipsilateral limb and saccadic movements intact. Neither visual hemifield bias nor visual attention deficits were observed. Thus our results are consistent with a motoric rather than visual organization in PRR, despite its early location in the visuomotor pathway. We found no effects on the temporal coupling of coordinated saccades and reaches, suggesting that this mechanism lies downstream of PRR. In sum, this study clarifies the role of PRR in the visuomotor hierarchy: despite its early position, it is a limb-specific area influencing reach planning and is positioned upstream from an active eye-hand coordination-coupling mechanism.

parietal reach region; reaching; visuomotor; eye-hand coordination

VISUOMOTOR TRANSFORMATIONS involve multiple brain areas with different functional organizations. Early visual areas process information from contraversive visual space, without respect to how that information will be used (hereafter, "visual organization"). In contrast, late motor areas do not parse information according to visual field but rather, encode movement-related information for effectors on the contralateral side of the body (hereafter "motor organization"). Whereas the poles of this pathway have been well characterized, we focus on a region involved early in the transformation from sensory to motor organization.

The parietal reach region (PRR), encompassing portions of macaque V6A and medial intraparietal (MIP) areas in the posterior and medial portion of the intraparietal sulcus (IPS), is situated early in the dorsal visuomotor pathway (Colby et al. 1988; Galletti et al. 1999). It receives direct input from extrastriate visual areas (Galletti et al. 2001; Gamberini et al. 2009; Johnson et al. 1996; Passarelli et al. 2011) and projects to dorsal premotor cortex (PMd) (Johnson et al. 1996; Pandya and Seltzer 1982). PRR shows sustained activity when planning a reaching movement to a target (Cohen and Andersen 2000; Snyder et al. 1997), with more activity before movements of the contralateral limb compared with the ipsilateral limb. PRR also shows sustained activity when planning a saccade, although the activity is substantially less than that observed before a reach (Calton et al. 2002; Kutz et al. 2003; Quian Quiroga et al. 2006; Snyder et al. 2000). Its position early in the visual-processing hierarchy (Felleman and Van Essen 1991) indicates that PRR is one of the first cortical regions to play a role in planning reaches. Additionally, the combination of reach- and saccade-related responses may indicate a role in eye-hand coordination (Battaglia-Mayer et al. 2001; Dean et al. 2011, 2012; Pesaran et al. 2006). Finally, activity in association with targets for saccades and reaches could reflect a role of PRR in attentional processing, as has been suggested for the nearby lateral intraparietal (LIP) area, which is also active in association with targets for upcoming movements of the hand or eye (Gottlieb et al. 1998; Snyder et al. 1997; Wardak et al. 2002).

Although task-evoked activity is helpful for suggesting the function of brain areas, function can also be assayed using interventional, rather than observational, techniques. For example, lesion studies allow us to examine how an organism performs in the absence of a particular portion of the brain, providing clues as to the function of the lesioned tissue. It has been argued that lesion studies provide corroborative and arguably more direct evidence for function than recording studies (Wardak et al. 2002), although like any technique, these results must be interpreted with care. Large lesions of the medial bank of the IPS have suggested a role in reaching with the contralateral limb (Brown et al. 1983; Lamotte and Acuña 1978; Rushworth et al. 1997). The interpretation of these studies is complicated by the use of surgical lesions that may extend beyond the medial bank, for example, onto the gyral surface, or that may affect the underlying and unrelated fibers of passage. Furthermore, behavioral assessment typically occurred days after the surgery, allowing time for adaptive compensation to occur and potentially obscure the results. Aspiration lesions of the entire anterior bank of the parieto-occipital sulcus (POS), immediately contiguous with the medial bank of the IPS, provide still more evidence for a role of this region in reaching with the contralateral limb (Battaglini et al. 2002, 2003). However, none of these studies measured eye movements and therefore, could not address the issues of effector specificity or eye-arm coordination.

We studied the effect of focal, reversible inactivation on memory-guided reaches, saccades, eye-hand coordination, and

Address for reprint requests and other correspondence: E. A. Yttri, Dept. of Anatomy and Neurobiology, Washington Univ. School of Medicine, 660 S. Euclid, Box 8108, St. Louis, MO 63110 (e-mail: eric@eye-hand.wustl.edu).

visual attention (Fig. 1*A*). PRR was inactivated with muscimol, a $GABA_A$ agonist. To verify the location of each injection, we added manganese, an magnetic resonance (MR)-lucent contrast agent, to the inactivation solution and performed anatomical MRI following each session [Fig. 1*B*; see also Liu et al. (2010)]. Despite significant increases in firing rate in PRR before ipsilateral limb reaches and saccades, PRR inactivation effects were exclusive to the contralateral limb. Consistent with a preferential role in reach planning, rather than reach execution, reach reaction time (RT) was most clearly affected, with weak effects on movement trajectory, velocity, and endpoint. No visual hemifield bias was observed, as one would find following inactivation of a visual area. Additionally, there were no effects on covert visual search, suggesting that PRR does not contribute to visual attention, and no effects on eye-hand coordination.

MATERIALS AND METHODS

Three adult male macaque monkeys (*Macaca mulatta*) were trained to make eye and/or arm movements to targets on a vertically mounted, custom-built, infrared touch-screen, located at a comfortable reaching distance in front of the monkey. A second set of infrared beams was placed 8.6 cm in front of the screen to monitor the position of the hand in space, even when it was not in contact with the screen. Touch position on the screen and hand position in space were each recorded at every 2 ms, with 3.5 mm resolution. Visual stimuli were back projected onto the touch screen. Eye movements were monitored with a scleral search coil (CNC Engineering, Enfield, CT). Hand position was recorded every 2 ms, with 3.5 mm resolution. Animals sat in complete darkness with their heads restrained in custom-made primate chairs (Crist Instrument, Hagerstown, MD). The fronts of the chairs were completely open so that the animals had free range of movement of the forelimbs. All procedures were in accordance with the *Guide for the Care and Use of Laboratory Animals* and were approved by the Washington University Institutional Animal Care and Use Committee.

Behavioral tasks. All animals performed memory-guided, center-out saccades. *Monkeys G*, *Q*, and *W* performed combined reaches and saccades ("coordinated reaches"). *Monkey G* performed reaches without saccades ("dissociated reaches"; Fig. 1*A*). Reach and saccade trials were interleaved. A Plexiglas panel blocked the arm not in use. Trials started with the animal fixating and touching a central fixation cue (5.5° windows for the eye; 6° for the hand). After 350 ms of fixation, a peripheral target was flashed for 150 ms in one of eight equally spaced locations, 20° (6.2 cm) from the fixation point. After a subsequent 1,000- to 1,600-ms delay, the fixation target was extinguished, and the animal had 500 ms to initiate and complete a saccade and/or 750 ms to initiate and complete a reach to within 10° of the remembered target location. On coordinated trials, reaches were initiated an average of 71.5 ms after the onset of the saccade. On dissociated trials, the nonmoving effector was constrained to a 5.5° central fixation window. All windows were kept large in both time and space so that lesion effects would not prevent the animals from performing the task. If the animal moved to within 10° of the target, a fluid reward was given. If the initial movement landed within 5.0° of the saccade target or 6.5° of the reach target, a second reward was given, and the trial was ended. If not, the target reappeared 150 ms after the completion of the initial movement, and the animal had up to 2 s to make a corrective movement to within 5.0° (saccade) or 6.5 (reach) of the (visible) target. Upon completion of a corrective movement, a second, smaller reward was given. Only the initial movement endpoint was used in data analysis; corrective movements to the visible target, along with the reward structure of the task, were used only to encourage the animals not to take advantage of the large windows but instead, to move as accurately as possible. Animals performed ~1,000 trials/session. One-half of these trials was dissociated saccade trials, and the other one-half was either coordinated reach with saccade trials or dissociated reach trials. Unless otherwise noted, "saccade" refers to dissociated, saccade-only trials.

Covert attention was assayed using a visual search task adapted from Wardak et al. 2002 (see Fig. 7*A*). Animals fixated a central fixation target. After a variable delay period of 800–1,300 ms, one purple square and seven purple distractors of varying shape appeared. All eight stimuli were equally spaced and 12° eccentric to the fixation point. In one-third of the trials, only the purple square appeared. Animals were rewarded for making a single saccade to within 6° of the square target. Trials in which saccades were made to a distractor or more than one saccade was performed were terminated immediately and counted as errors. The difference in RT and error rate on trials with and without distractors served as a measure of covert attention (Liu et al. 2010; Wardak et al. 2002, 2004).

Reaches were defined as a change in hand position of at least 3° of visual angle. Reach onset and offset were defined as the time at which

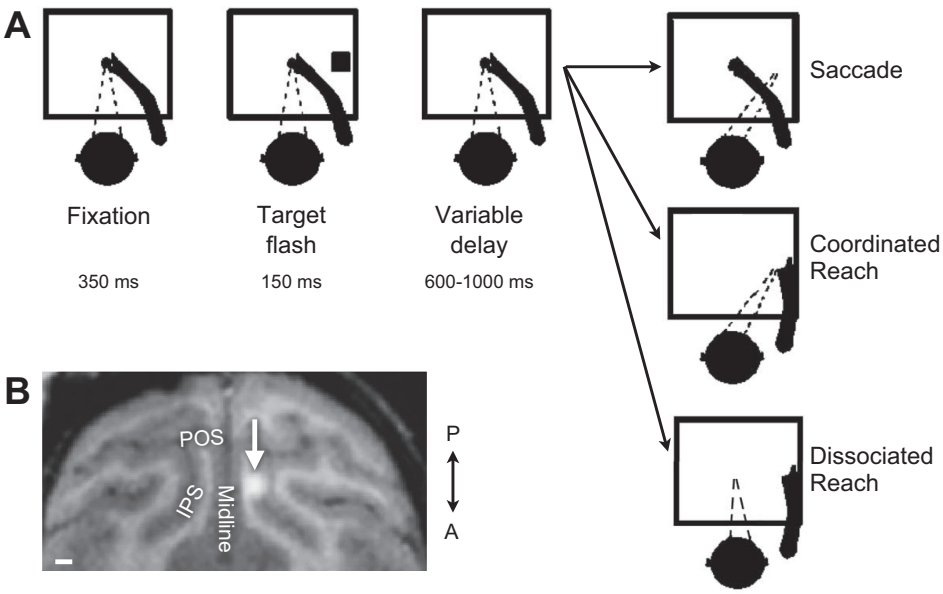

Fig. 1. Experimental setup. *A*: behavioral task. After an initial fixation period, a target briefly appeared at 1 of 8 peripheral locations. The target color instructed both movement type and location: green for reach and red for saccade (color not shown in figure). After a variable delay period, the central fixation point disappeared, cueing the animal to make a saccade, dissociated reach, or coordinated reach and saccade to the remembered target. Saccade-alone trials were interleaved randomly with either dissociated or coordinated reach trials. *B*: horizontal magnetic resonance (MR) image taken from a representative parietal reach region (PRR) injection. The bright white region indicates the location of the muscimol plus manganese injection (1 μl) into the medial bank of the intraparietal sulcus (IPS). POS = parieto-occipital sulcus; P = posterior; A = anterior. Scale bar = 2 mm.

the arm moved 1° from the starting or ending position, respectively. Animals often remained in contact with the touch screen, especially during the initial portion of the reach. If the hand left the screen without first moving along it, then reach onset was defined as the time of leaving the screen. Saccades were defined as a change in eye position of at least 2°. Saccade onset and offset were defined as the time at which the velocity increased to 20°/s or decreased to 16°/s, respectively. Within each session, accuracy and precision (endpoint scatter) were computed for each target location. Accuracy was quantified as the Euclidian distance between the target and the mean endpoint. With the comparison of mean accuracy in this way—before and after inactivation—we are sensitive to systematic effects in any direction, e.g., hypometria, hypermetria, leftward or upward shifts, clockwise deviations, etc. We also tested separately for hypometria/hypermetria, using more specific tests that would have greater statistical power. We report all distance-based results in degrees of visual angle for consistency; the conversion to linear distance, of course, depends on distance of the touch screen from the eyes (typically 17 cm).

Trial-by-trial endpoint scatter was used as a measure of movement precision and quantified as the average Euclidian distance between each individual movement endpoint and the mean endpoint. Errors included movements that occurred before or after the allotted movement period, failure to maintain fixation at the location of the peripheral target for at least 150 ms, movements that landed more than 10° away from the remembered peripheral target location, or failure to make a corrective movement to the peripheral target location after it flashed at the end of the trial. Trials in which an error occurred before the initial target appearance were excluded from the study.

Behavioral data from each inactivation session were compared with the data from the two previous control sessions. Unless otherwise noted, statistical significance was computed using a Student's *t*-test. The significance of inactivation effects across sessions was computed using a paired two-tailed Student's *t*-test. We used a paired *t*-test rather than a pooled *t*-test for this comparison so that differences in baseline values across individuals would not influence our computation of significance. The significance of the effect of each inactivation vs. the two previous control sessions was computed using a two-tailed Welch's *t*-test, which allows for different variance in the control and injection data and is more conservative than a standard Student's *t*-test.

To compare reach trajectories, hand position was measured at 2-ms intervals throughout each reach. The samples were normalized to a constant duration by dividing the time of each sample, relative to the start time of the reach, by the total reach time. The data were then averaged by direction to form 48 mean trajectories (control and inactivation trajectories for three animals and eight directions). For each inactivation-control pair, the largest deviation occurring within the first half of the trajectory was identified. Statistical significance was determined using a permutation test, in which trials were reassigned randomly as injection or control, and maximum deviation was recomputed. This was repeated 1,000 times, and the significance was determined by the rank order of the actual deviation within these shuffled deviations.

Reversible inactivation. PRR was identified and localized with a single-unit recording, assisted by anatomical MR images. Injections were placed within the medial bank at approximately 6–8 mm behind the interaural line, 5 mm lateral, and between 4 and 6 mm below the surface of the brain. For each inactivation, a cannula was lowered to the desired position. Next, 0.5–2.0 μl (most were 1.4 μl or less) of 8 mg/ml muscimol and 0.1 M of the MRI contrast agent manganese [19.8 mg/ml $MnCl_2(H_2O)_4$] were injected through a 33-g cannula (Small Parts, Logansport, IN) at a rate of 0.05–0.15 μl/min (microinjection pump; Harvard Apparatus, Holliston, MA). The cannula was left in place for 10 min after the completion of the injection and then was retracted slowly. In three sessions, we recorded spontaneous and task-evoked activity from 1 mm away from the point of injection and found nearly complete suppression of activity, confirming the efficacy of the inactivation (data not shown).

Control sessions were identical to inactivation sessions in number of trials, time, and tasks performed. In control sessions, the injection microdrive was mounted on the monkey's head, and the microinjection pump ran with the same timing as in an injection session, but the cannula was not lowered into the brain. The two behavioral sessions preceding each inactivation were used as control sessions, which never occurred on the day following an inactivation, and inactivation sessions were spaced at least 4 days apart. Control sessions did not include saline or manganese injections. We are interested in the effects of a localized dysfunction, regardless of whether that dysfunction is caused specifically by $GABA_A$ inactivation or by a nonspecific effect, such as a focal increase in pressure. Note, however, that we have shown previously that injecting a manganese alone into the parietal cortex does not affect behavior (Liu et al. 2010) and that inactivation of the nearby LIP area induced saccade-specific deficits in the same task, while leaving reaches unaffected (Yttri et al. 2013).

Lesion localization. Two to 4 h after each injection, after collecting the behavioral data, T1-weighted anatomical images were obtained using a magnetization-prepared, rapid-acquisition gradient echo sequence, conducted at 0.5 mm^3 on a 3T head-only MRI system (Siemens Allegra; Siemens, Malvern, PA). A single-surface coil was used. Animals were head restrained and lightly sedated with ketamine (3 mg/kg) during the procedure. Injections were visible as a bright halo representing the manganese-induced T1 signal increase. Only those injections centered in the posterior portion of the medial bank of the IPS and the contiguous portion of the anterior bank of the POS were included in this study. Injections that spread across the POS and into the anterior bank or across the IPS and into the lateral bank were excluded. Exclusions were based only on injection location; no experimental sessions were excluded based on behavioral results.

RESULTS

To examine the role of PRR in the visuomotor pathway, we reversibly inactivated PRR in three monkeys in 28 separate injection sessions. We were particularly interested in whether the spatial organization of PRR more closely resembles that of visuosensory or motor cortex. For each experiment, lesion location was confirmed by MRI of co-injected manganese (see MATERIALS AND METHODS). We measured the inactivation-induced changes in performance, including effects on RT, movement duration, accuracy, and endpoint scatter (inverse precision), in interleaved, memory-guided saccade and reach trials. Reaches were accompanied by eye movements in some experiments and dissociated in others. The effects of PRR lesions on coordinated and dissociated movements are very similar (see below), and so, these data are combined together in the first half of the paper. Because of the similarity in effects across these conditions, the data are combined here but will be examined individually later in the manuscript.

Across sessions, muscimol injection into PRR slowed the RT of reaches performed with the contralateral limb by 6.8 ms ($P = 0.000043$, two-tailed *t*-test; Fig. 2*A*). In contrast, there was no effect of inactivation on reach RT performed with the ipsilateral limb (mean = −0.6 ms, $P = 0.72$) or on saccade RT (mean = −1.2 ms, $P = 0.2$).

The contralateral limb effect is highly significant but small compared with the mean RT (259 ms). However, reach RTs are tightly clustered. Cohen's d is the ratio of an effect size to the SD of the control value. This ratio expresses how large the effect is compared with the variability of the quantity being measured and depends only on the characteristics of the be-

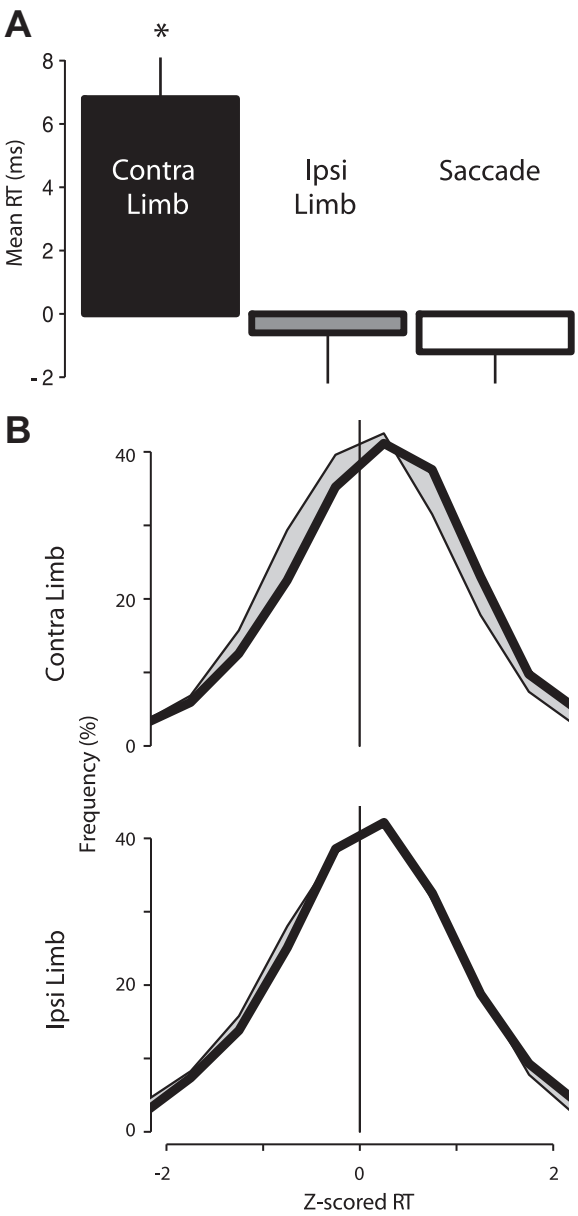

Fig. 2. Effect of PRR inactivation on reaction time (RT). *A*: mean and SE are shown for each effector in the memory-guided movement task (*$P < 0.05$, 2-tailed *t*-test). Lesion effects are specific to contralateral reaches. *B*: histogram of Z-scored RTs for each effector. Control (thin lines) and inactivation (thick lines) show distribution of data for contralateral (Contra; *top*) and ipsilateral (Ipsi; *bottom*) limb movements. Shaded regions represent differences in distributions. Data were Z scored by animal and reach direction.

havior itself. Consider the impact of a 1-s advantage in a race. If most racers finish within seconds of one another, then a 1-s advantage will have a huge impact, regardless of whether the mean time to complete the race is measured in seconds, minutes, or hours. Cohen's d captures this by computing the observed change divided by the SD of the baseline measurement. (Note that this differs from a *t* statistic, which is the ratio of the observed change divided by the SE of the mean. The *t* statistic depends on the number of measurements that is made and thereby confounds effect size with experimental design.) The RT effect sizes, as measured by Cohen's d, are 0.26, 0.33, and 0.35 for *monkeys G*, *Q*, and *W*, respectively. With the assumption of normally distributed data and similar pre- and postinjection SDs, this means that a randomly drawn postinjection RT would be slower than a randomly drawn control RT on ~60% of trials. Thus whereas the effect size that we observed was only 3% of the mean RT, this numerically small effect comprised a substantial fraction of the normal variance and has a noticeable effect on behavior, even at the single-trial level.

The contralateral limb-specific increase in RT was observed across the entire spectrum of reaches rather than confined to some subpopulation of reaches (Fig. 2*B*). For instance, a small increase in the number of trials with very long latencies or a decrease in the number of trials with very short latencies could have produced the same mean effect. Instead, we found a highly systematic effect on reaches across latencies. However, the effects were confined to reaches with the contralateral limb; reaches with the ipsilateral limb did not demonstrate any change in their RT distribution.

Lesion effects did not depend on the spatial location of the target for the movement. Figure 3 depicts the mean effect of inactivation on RT for each of the eight targets. Reaches with the contralateral limb were slowed, independent of target

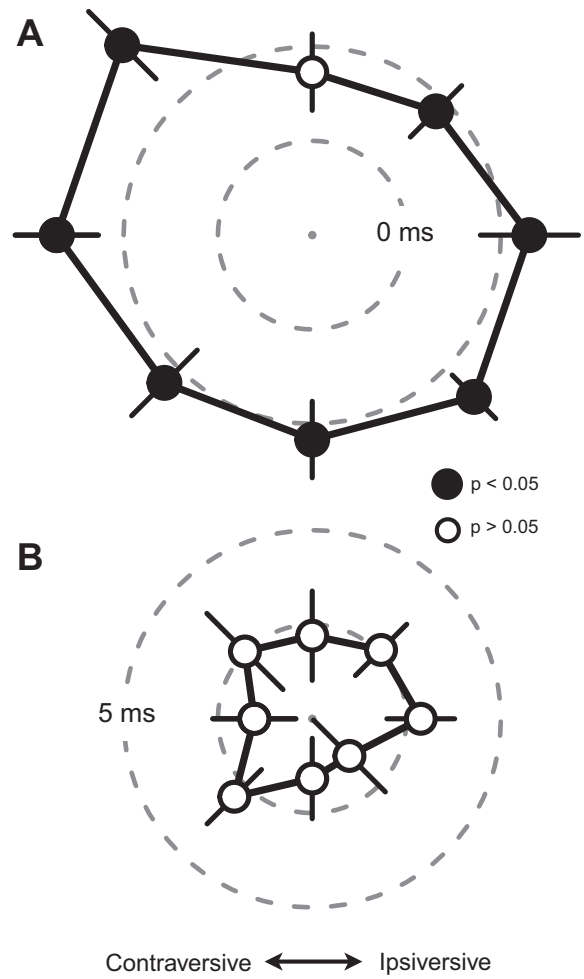

Fig. 3. Polar plot of the inactivation effect on reaches with the contralateral (*A*) or ipsilateral (*B*) limb to each of 8 targets. The inner, dashed circle represents no effect; the outer, dashed circle represents a 5-ms slowing of RT. The central point represents a 5-ms speeding of RT. Significance ($P < 0.05$, 1-tailed *t*-test) is indicated by filled data points. Data from *monkey G* were right-left flipped, such that the contraversive visual field falls on the right for all 3 animals.

Table 1. *Mean control reaction times (RTs) and inactivation-induced changes for individual animals*

Monkey (*n*, side of inactivation)	Contralateral Limb RT		Ipsilateral Limb RT		Saccade RT	
	Control	Effect	Control	Effect	Control	Effect
G (9, right)	**212.2**	**4.5 ± 1.2**	208.7	−0.2 ± 1.2	192.2	−1.1 ± 1.1
Q (13, left)	**270.4**	**7.4 ± 1.8**	272.0	−2.3 ± 2.8	201.5	−0.4 ± 1.6
W (6, left)	*302.8*	*9.0 ± 4.1*	276.9	2.6 ± 4.2	229.0	−2.2 ± 2.5
All (28)	**258.6**	**6.8 ± 1.4**	252.6	−0.6 ± 1.5	205.6	−1.2 ± 0.9

RTs (mean ± SE) are shown in milliseconds. Bold values indicate significant inactivation effects ($P < 0.05$, 2-tailed *t*-test). Italics represent trends ($P < 0.15$).

direction ($P < 0.05$ for seven of eight directions, one-tailed *t*-test; $P = 0.52$, Rayleigh's test for uniformity). There was no significant difference in RT for reaches made to targets in the contraversive vs. ipsiversive hemifields (slowing of 7.8 vs. 6.2 ms, difference of 1.6 ms, $P = 0.29$, two-tailed paired *t*-test). Reaches made with the ipsilateral limb, by contrast, were neither slowed down nor sped up for any target direction ($P > 0.2$ for each individual direction, two-tailed *t*-test).

This pattern of effects—a slowing of reaches specific to the contralateral limb but not specific for reaches into either visual hemifield—was also seen at the level of individual inactivations. Slowing was greater for the contralateral compared with ipsilateral limb in 23 out of 28 experiments, with a significant difference ($P < 0.05$, two-tailed *t*-test) in 18 experiments. Slowing was significantly greater in the ipsilateral limb in only two experiments. In contrast to these limb-specific effects, there were no field-specific effects. Slowing after inactivation was nearly equal for targets in each field, with greater effects for the contraversive targets in 13 of 28 experiments (not different from chance, $P = 0.7$, χ^2 test). There were significant differences between reaches to the two hemifields in only three experiments. Across sessions, there was no correlation between the limb and hemifield effects; that is, it was not the case that inactivations eliciting stronger effects on the contralateral arm showed stronger effects in the contralateral visual field (Pearson's r = −0.06, $P = 0.8$).

This pattern of effects was also consistent across individual animals. Reaches with the contralateral limb were slowed by 4.5, 7.4, and 9.0 ms in each of the three animals (G, Q, and W, $P = 0.0057$, 0.00085, and 0.079, respectively). There was no effect on ipsilateral reaches ($P > 0.5$) or saccades ($P > 0.3$) in any individual animal (Table 1). In no case was there a significant difference in the effects between hemifields. Mean saccade latency was reduced in each individual, but in no case was the reduction significant for saccades.

Other movement parameters showed similar specificity for reaches with the contralateral limb (Tables 2 and 3). Inactivation caused a significant slowing of contralateral limb velocity (3.6°/s, $P = 0.026$) but not ipsilateral limb or saccade velocity (0.8°/s and 0.2°/s, respectively). Inactivation also caused a small but significant increase in movement duration (4.1 ms, $P = 0.031$) and decrease in reach accuracy (0.2° increase in the average disparity between mean endpoint and target, $P = 0.025$). The effect on accuracy was not significant when a more conservative permutation test was applied ($P > 0.3$). Again, none of these parameters (velocity, accuracy, duration) was affected significantly for reaches with the ipsilateral limb or saccades. Endpoint scatter was not increased significantly for either limb. Finally, we found no significant hypometria or hypermetria (Table 4). Contralateral reaches exhibited a trend toward hypometria, and ipsilateral reaches trended toward hypermetria, but the magnitudes of these effects were small (~1%).

Inactivation had subtle effects on contralateral but not ipsilateral limb trajectories. We scaled each reaching movement to a fixed duration and then averaged movements to each target for each animal. Figure 4 shows the average control and postinjection reach trajectories for each limb obtained from *monkey Q*. Across animals, we found significant divergence in nine of 24 postinjection trajectories (eight directions for each of three monkeys) for the contralateral limb and in three of 24 trajectories for the ipsilateral limb (see MATERIALS AND METHODS). The contralateral limb results exceed what would be expected by chance ($P = 1E\text{-}6$, computed from a binomial distribution with a 5% chance of each individual event), whereas the ipsilateral limb results do not differ from chance ($P = 0.12$).

PRR inactivation does not affect the temporal aspects of eye-arm coordination. Humans and nonhuman primates typically move their eyes when they reach, with gaze arriving on target shortly before the reach is completed [Biguer et al. 1982; Dean et al. 2011; Prablanc et al. 1979; Rogal et al. 1985; but see Abrams et al. (1990) and Ballard et al. (1992)]. The movement onset times (RT) for coordinated saccades and

Table 2. *Effects of parietal reach region inactivation*

	Contralateral Limb		Ipsilateral Limb		Saccade	
	Control	Effect	Control	Effect	Control	Effect
RT, ms	**258.6**	**6.8 ± 1.4**	252.6	1.1 ± 1.5	205.6	−1.2 ± 0.9
Mean velocity, degree/s	**118.1**	**−3.6 ± 1.5**	122.2	0.8 ± 2.0	310.2	0.2 ± 3.6
Duration, ms	**123.3**	**4.1 ± 2.1**	116.0	−0.2 ± 2.5	62.8	−0.1 ± 0.5
Amplitude, degree	*18.3*	*−0.2 ± 0.1*	18.4	0.2 ± 0.1	*18.8*	*−0.2 ± 0.1*
Endpoint scatter, degree	*4.8*	*2.1 ± 1.3*	5.12	0.9 ± 1.2	3.4	−0.6 ± 0.6
Accuracy, degree	**5.7**	**0.2 ± 0.1**	*5.90*	*0.1 ± 0.1*	3.8	0.1 ± 0.1

Values for mean ± SE are presented for RT, velocity, duration, amplitude, endpoint scatter, and accuracy, averaged across 3 animals. Bold values indicate significant inactivation effects ($P < 0.05$, 2-tailed *t*-test). Italics indicate trends ($P < 0.15$, 2-tailed *t*-test).

Table 3. *Inactivation effects (mean ± SE) for each animal for 6 parameters*

	Monkey Q, n = 13		Monkey W, n = 6		Monkey G, n Coordinated = 2		Monkey G, n Dissociated = 9	
	Contra	Ipsi	Contra	Ipsi	Contra	Ipsi	Contra	Ipsi
RT, ms	**7.4 ± 1.8**	−2.3 ± 2.8	**9.0 ± 4.1**	2.6 ± 4.2	4.3 ± 2.0	0.3 ± 1.3	**4.5 ± 1.2**	−0.2 ± 1.2
Mean velocity, degree/s	**−6.7 ± 2.7**	0.8 ± 4.6	−1.1 ± 2.2	0.5 ± 3.9	2.1 ± 2.3	0.9 ± 2.1	*−3.1 ± 1.8*	0.6 ± 2.0
Duration, ms	**7.1 ± 3.0**	−0.1 ± 4.6	1.5 ± 2.1	−0.3 ± 3.1	2.4 ± 3.5	−0.2 ± 2.0	**2.6 ± 1.8**	−0.2 ± 1.7
Accuracy, degree	0.1 ± 0.1	0.1 ± 0.2	**0.4 ± 0.1**	0.2 ± 0.1	0.1 ± 0.0	0.0 ± 0.1	*0.3 ± 0.1*	0.1 ± 0.1
Amplitude, degree	−0.1 ± 0.2	0.2 ± 0.2	*−0.3 ± 0.1*	0.1 ± 0.1	−0.2 ± 0.2	0.1 ± 0.1	−0.1 ± 0.1	0.2 ± 0.1
Endpoint scatter, degree	2.1 ± 1.8	−0.2 ± 1.2	2.3 ± 1.7	0.3 ± 2.1	1.5 ± 2.9	3.1 ± 3.2	*2.2 ± 1.3*	2.0 ± 1.7

Monkey G is listed twice, with 1 set of entries for coordinated reaches and a 2nd set for dissociated reaches. Reaches with the contralateral limb are shaded in gray. Bold values indicate significant inactivation effects ($P < 0.05$, 2-tailed t-test). Italics indicate trends ($P < 0.15$, 2-tailed t-test). Contra, contralateral; Ipsi, ipsilateral.

reaches are correlated on a trial-by-trial basis (Dean et al. 2011, 2012; Fischer and Rogal 1986; Fisk and Goodale 1985; Snyder et al. 2006). If PRR plays a functional role in the temporal coordination of eye and limb movements, then PRR inactivation should decrease this correlation. This was not the case. Figure 5*A* shows that PRR inactivation had no significant effect on the correlation between eye- and limb-movement RTs [contralateral limb: control r = 0.35, inactivation r = 0.34, P = 0.7, Fisher r-to-z transformation test; ipsilateral limb (data not shown): control r = 0.45, inactivation r = 0.46, P = 0.8, Fisher r-to-z transformation test]. This absence of an inactivation effect on eye-arm correlations remained when the data were restricted to movements into the contraversive field ($P > 0.6$), as well as when the data were restricted to just those sessions with significant increases in reach RTs ($P > 0.4$). Finally, there was no consistent pattern of change in eye-arm correlation within each individual animal. The control and experimental correlations changed from 0.35 to 0.32 (*monkey Q*, $P > 0.5$), from 0.34 to 0.37 (*monkey G*, $P > 0.7$), and from 0.42 to 0.43 (*monkey W*, $P > 0.7$).

It is possible that an effect on coordination could be masked by analyzing across sessions. To determine if there was an effect within individual injections, we determined the correlation coefficient for saccade and reach RT for each inactivation. There was no difference between inactivation and control sessions in their average correlation (mean r value = 0.36 for both, SE = 0.03 for both, $P > 0.9$ permutation test). Furthermore, larger injections did not produce larger effects. Across individual sessions, there was no correlation between the degree of saccade and reach RT correlation and the injection volume (between 0.5 and 3.0 μl; r = 0.04, P = 0.87).

Thus we found that although PRR inactivation slows reaches but not saccades (Fig. 2), there is no change in the correlation between saccade and reach RTs (Fig. 5*A*). This may seem paradoxical; however, in mathematical terms, the correlation between a set of x and y values is not changed by adding a constant to all of the x values. In other words, PRR inactivation introduces a roughly constant offset into the relative timing between the reach and saccade but does not otherwise change the pattern of eye-arm coupling that emerges across trials.

We undertook a second analysis to test the conclusion that although PRR inactivation slowed limb movements but not eye movements, inactivation did not affect the temporal coupling of the eye and arm. This analysis was based on the variability of movement times. We considered the trial-by-trial variability of the lag between saccade and reach onset times. In the control condition, the data demonstrate that reaches and saccades are not initiated independently. If reaches and saccades were initiated independently, then $(SD_{lag})^2 = (SD_{saccade})^2 + (SD_{reach})^2$. Instead, the SD of the lag (the difference between contralateral limb reach and saccade RT values) was 24% less than what would be predicted if independent processes determined reach and saccade RTs (Table 5). This reduction of variance is evidence of coordination. However, this coordination could arise due to an active process of eye-arm coordination, a passive effect of a common input, or both factors. If the coordination is mediated, in part, by PRR, then a PRR lesion should cause the observed SD of the lag to move closer to the prediction of independent processes. This is not what we found.

Following inactivation, saccade variability was unaffected (control SD = 26.4; inactivation SD = 26.7; P of effect = 0.49, F-test), but reach variability was increased significantly (control SD = 33.7; inactivation SD = 36.0; P of effect = 0.0002, F-test). The variability of the lag was also increased significantly (SD = 34.4; P of difference = 0.0004, F-test). This increase, manifest as a decrease in the slope in the cumulative distribution (Fig. 5*B*), could reflect either a disruption of eye-arm coordination or a reach-specific deficit. In the absence of a coordination mechanism, the predicted SD of the lag is 44.8 ms; the observed value was 34.5 ms. This represents a 41% reduction from the expected variance, which is not significantly different from the 43% reduction observed in the control data (P = 0.69). From this, we can conclude that PRR inactivation increases the variability of reach but not saccade

Table 4. *Movement amplitude by visual hemifield*

	All Targets		Contraversive Field		Ipsiversive Field	
	Control	Effect	Control	Effect	Control	Effect
Contralateral limb	*18.3*	*−0.20 ± 0.13*	19.2	0.14 ± 0.20	*17.5*	*−0.50 ± 0.26*
Ipsilateral limb	*18.4*	*0.17 ± 0.10*	17.8	0.07 ± 0.16	18.9	0.26 ± 0.20

Values for mean amplitude ± SE are presented in degrees for each visual field. Bold values indicate significant inactivation effects ($P < 0.05$, 2-tailed t-test). Italics indicate trends ($P < 0.15$, 2-tailed t-test).

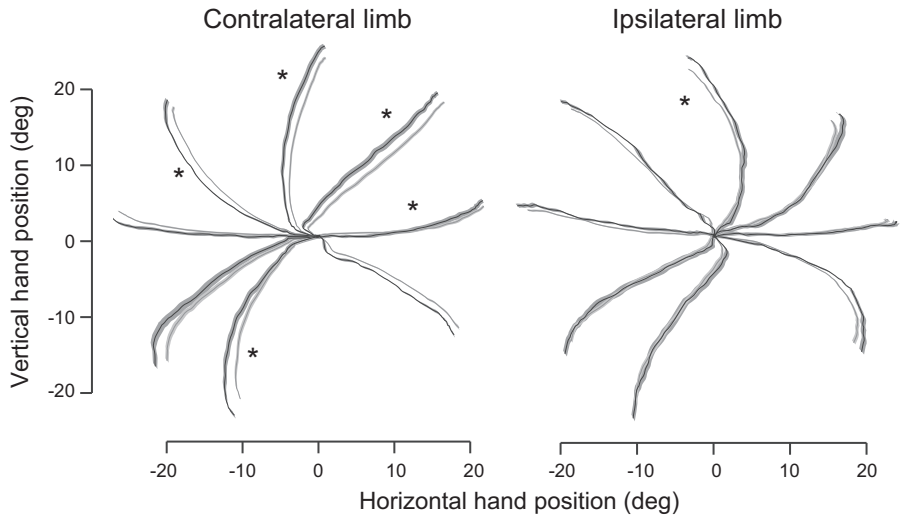

Fig. 4. Effect of PRR inactivation on reach trajectories. The mean trajectories for contralateral (*left*) and ipsilateral limbs (*right*) are plotted for control (gray) and inactivation (black) trials (shaded region is ±1 SE). *Trajectories with significant deviation ($P < 0.05$; see MATERIALS AND METHODS) in the 1st half of the reach. The contraversive visual hemifield is located on the left side (negative horizontal values) of each panel.

RTs, consistent with an effector-specific role in reaching, but does not affect the mechanism responsible for temporal coupling between coordinated eye and arm movements. This is strong evidence that the coordination of saccade and reach timing is not dependent on an intact PRR.

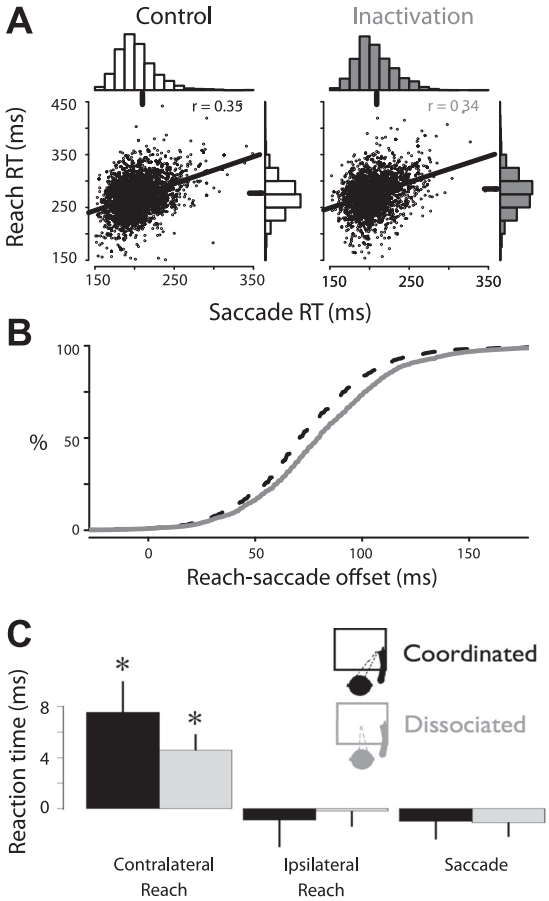

Fig. 5. PRR inactivation does not affect temporal eye-arm coordination. *A*: coordinated saccade (abscissa) and reach (ordinate) movement latencies are plotted for each trial from control (*left*) and inactivation (*right*) sessions. *B*: cumulative histogram of reach-saccade RT offsets for control (dashed line) and inactivation (solid line) trials. *C*: bar plot of inactivation effect on each effector during coordinated (black) and dissociated (gray) movements. *$P < 0.05$, 2-tailed *t*-test.

A third line of evidence is also consistent with this conclusion. Figure 2 contains data from coordinated reaches plus saccades, as well as from dissociated reaches, each made in isolation of the other. If PRR helps mediate eye-arm coordination, then we would expect that a PRR lesion would have differential effects on coordinated compared with isolated movements. Instead, we find no difference in the effects of inactivation when coordinated and dissociated movements are compared (Fig. 5*C*). For the contralateral limb, coordinated and dissociated reach RTs were slowed by similar amounts (7.5 and 4.5 ms, respectively; P of difference = 0.3). For the ipsilateral limb, neither coordinated nor dissociated reaches were slowed significantly (−0.9 and −0.2 ms, respectively; $P > 0.6$ in either case; P of difference = 0.8). Finally, neither dissociated nor coordinated saccades were slowed significantly by inactivation (−1.0 and −1.1 ms, respectively; $P = 0.9$). In two experiments, both coordinated and dissociated movements were performed within the same session. In those cases, the effect of PRR inactivation on coordinated and dissociated reach RT differed by only 0.2 ms (4.3 and 4.5 ms, respectively; $P = 0.9$, paired *t*-test). There was also no difference between the coordinated and dissociated reaches within these sessions ($P > 0.5$ in each case). The fact that the inactivation has indistinguishable effects on coordinated and dissociated eye and arm movements provides further evidence that PRR does not play a role in coordinating eye and limb movements.

PRR lesions do not impair a covert visual search. Posterior parietal cortex and in particular, area LIP have been implicated

Table 5. *SD in milliseconds for RTs of reaches, saccades, and the SD of the lag (reach RT − saccade RT for each trial)*

	Control	Inactivation	Difference
Reach SD	33.7	36.0	2.3
Saccade SD	26.4	26.7	0.3
Predicted lag SD	42.9	44.8	1.9
Actual lag SD	32.4	34.5	2.1
Reduction in variance (SD^2; actual vs. predicted)	−43%	−41%	+2%

Predicted SD values are computed based on the hypothesis of independent reach and saccade RTs, in which case, variances will add. Reductions in actual variability may reflect both passive as well as active eye-hand coordination mechanisms.

in directing attention to salient targets (Gottlieb et al. 1998; Liu et al. 2010; Wardak et al. 2002, 2004); for review, see Bisley and Goldberg (2010). We tested PRR for its role in attention using an attention-demanding, covert visual search task (Fig. 6*A*). We used the same paradigm and analysis as Wardak et al. (2002), in which trials, with and without distractors, are contrasted. Animals must make one and only one saccade to the target to indicate the result of their search. The RT and error rate in trials without distractors are subtracted from search trials to remove any oculomotor effects from this measure of attention.

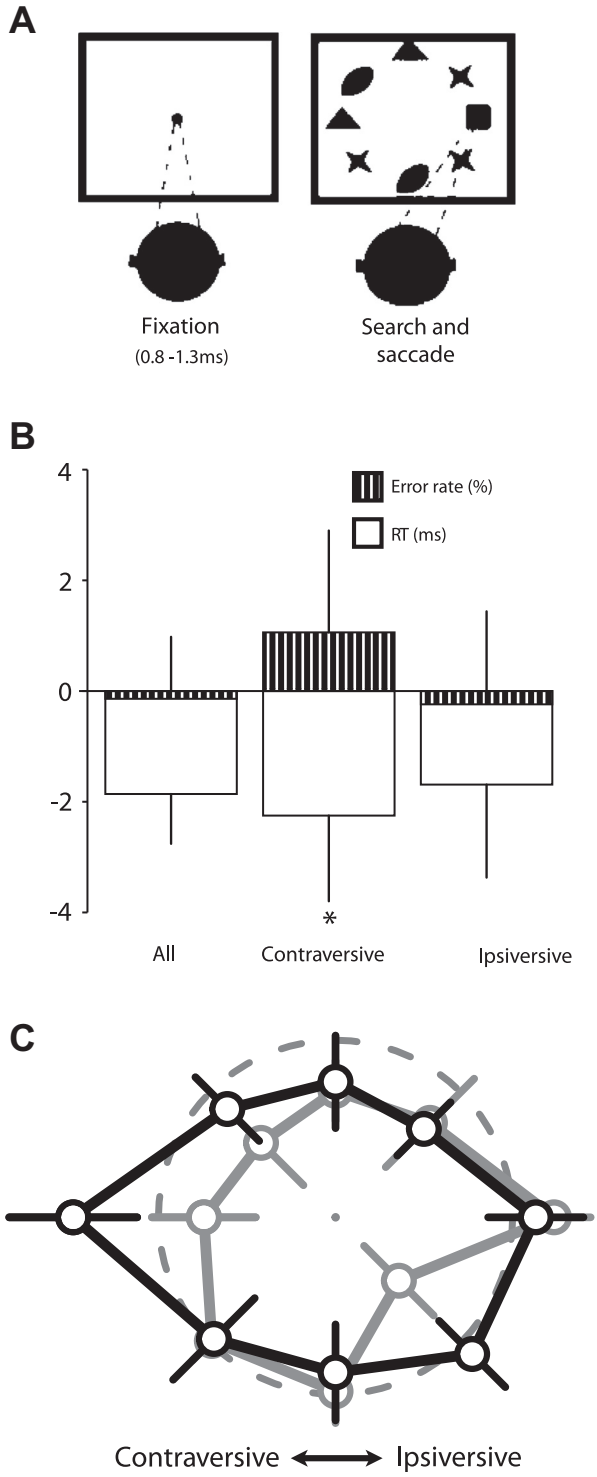

Fig. 6. Effect of PRR inactivation on visual search task. *A*: visual search task used to probe covert attention. Monkeys performed a single saccade as quickly as possible to the target (square) upon presentation of 8 visual stimuli. *B*: mean changes in error rate (striped) and RT (white) are shown for all targets (*left*; includes targets at top and bottom); only contraversive field targets (*middle*); and only ipsiversive field targets (*right*). Error bars represent SE. Only the improvement in RT for all targets was statistically significant ($P < 0.05$, 2-tailed *t*-test). For both measures, performance for target-only conditions (1/3 of trials; not shown) was subtracted from that in 7 distractor trials to control for possible motor deficits. *$P < 0.05$, 2-tailed *t*-test. *C*: polar plot of the inactivation effect on RT (gray) and error rate (black) to each of 8 targets. The dashed circle represents no effect; the inner point represents a 5-ms speeding or a 1% increase in performance, respectively. No individual direction achieved significance ($P < 0.05$, 1-tailed *t*-test).

Inactivation of PRR did not impair performance in this task (Fig. 6, *B* and *C*). We observed no significant change in error rate (all targets: −0.1%, $P = 0.88$; contraversive targets: 1.1%, $P = 0.57$; ipsiversive targets: −0.2%, $P = 0.87$). If anything, PRR lesions produced a moderate speeding effect for search RT (all targets: −1.9 ms, $P = 0.044$; contraversive targets: −2.3 ms, $P = 0.16$; ipsiversive targets: −1.7 ms, $P = 0.33$). It is possible that these modest effects may be due to a release of an inhibitory influence of PRR. The target of that inhibition could be LIP, although at this time, this is speculative. Attention has been shown previously to interact negatively with motor activity, decreasing activity in primary motor cortex, even in simple tasks, such as finger-tapping (Milnik et al. 2013) or walking (Al-Yahya et al. 2011). In comparison, ventral LIP lesions, tested in our laboratory using identical procedures, produced substantial deficits in both RT and percent correct, particularly for contraversive targets (Liu et al. 2010). These results confirm that PRR does not play a role in general visual attention or saccades but instead, contributes specifically to reach-related processes.

To confirm the location of our inactivation sites, we added manganese (0.1 M) to our inactivation solution and visualized each injection in vivo using MRI (Liu et al. 2010). Injection sites were reconstructed from anatomical MR images of the IPS and surrounding brain and then warped onto a three-dimensional atlas space (Caret, http://brainvis.wustl.edu, sum database: Macaque.F6.BOTH.Std-MESH.73730). Figure 7 contrasts injection sites and PRR recording sites from *monkey G*. The recording sites and injection sites are colocalized to the posterior end of the IPS and the anterior bank of the POS, covering portions of anatomical areas MIP and V6a.

Area MIP lies on the posterior portion of the medial bank of the IPS, whereas area V6a lies primarily on the anterior bank of the POS. Our injections covered portions of both areas. Although there are known cytoarchitectonic differences between the areas (Luppino et al. 2005), descriptions of V6a have emphasized the border with V6, whereas the border between MIP and V6a has been difficult to define [for review, see Cavada (2001)]. In practice, the border is often assigned to the anatomical boundary between the POS and IPS [e.g., Galletti et al. (1999)]. Yet, even the location of this anatomical boundary is uncertain. Some atlases simply label the medial bank of the IPS and the lateral half of the anterior bank of the POS as a single structure—the superior parietal lobule [BrainInfo (1991–present), National Primate Research Center, University of Washington, http://www.braininfo.org]. We find it difficult to place a lesion that is >2 mm in diameter wholly within the

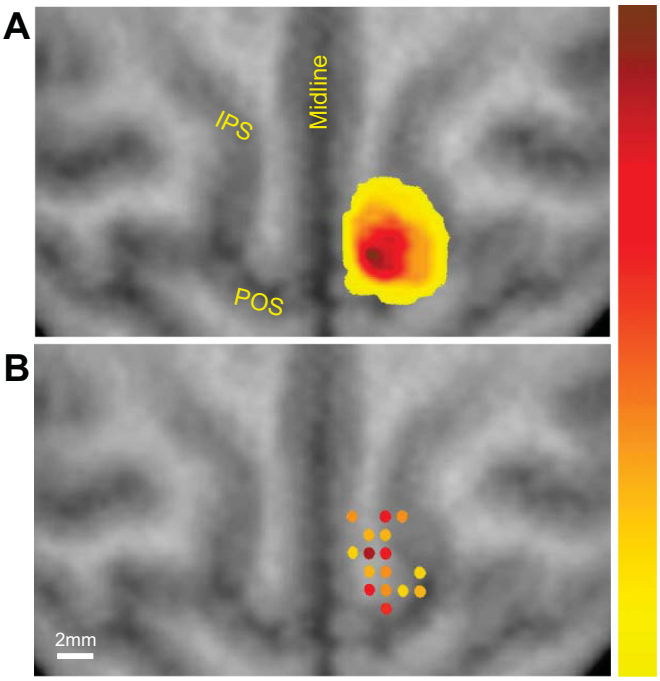

Fig. 7. Anatomical localization. *A*: individual injection halos from 1 animal (*monkey G*) were aligned and superimposed on a representative horizontal MR image plane. Darker colors signify greater overlap of individual inactivation halos, ranging from 1 (yellow) to 9 (dark red). *B*: location of PRR cells recorded from the same animal, aligned and superimposed on a single slice. Color-coding ranges from 1 (yellow) to 9 cells (dark red), although tracks where only 1 PRR cell was found are not shown. Electrode tracks were not orthogonal to the plane of the image, and as a result, there is some offset in the locations of cells recorded more than a few millimeters from this slice.

anterior bank of the POS, without also affecting the medial bank of the IPS, and we found no systematic difference in results between injections placed more anterior or posterior. Therefore, whereas it is possible that the effects that we observe are the result of the inactivation of MIP or V6a alone, we feel that the distinction would be difficult to make based on our MR images.

DISCUSSION

PRR is situated early in the visuomotor pathway, and its pattern of activity leaves its role ambiguous. Recording studies can demonstrate what signals are present and can suggest what computations may be carried out in a particular area. However, signals may be present that do not play a direct role in driving behavior. Reversible lesion studies help to identify these cases, although negative results must be interpreted with caution, since a loss of function in one area may be compensated by processes in other parts of the brain. With this caveat in mind, the current study reveals three major findings. First, although signals correlated with movements of either limb can be found in PRR, lesion effects are specific to contralateral limb movements. Second, the limb specificity and spatial organization of PRR are more congruent with motor than with sensory cortical areas. These two findings suggest that limb-specific movement planning occurs early in the visuomotor pathway. Finally, PRR does not appear to play a direct role in coordinating saccades and reaches.

The contralateral limb RT effects that we observed were extremely reliable within and across animals. Although small compared with overall RT, they were a significant fraction of the SD of that measure. We believe that the effect was small, because visually guided reaching is a robust, well-practiced behavior; we lesioned only a portion of PRR; or parallel and compensatory pathways for reaching are likely engaged, potentially including the intact PRR in the opposite hemisphere. In contrast to the clear, contralateral limb effects, we saw no effect on reaching with the ipsilateral limb, on saccades, or on visual attention.

PRR as a motoric region. We have shown that PRR represents information from either visual hemifield and routes this information toward pathways that eventually control muscles on the contralateral side of the body. In combination with the specificity for the contralateral limb, this is more consistent with the spatial organization of a cortical motor area than that of a visual sensory area. In the cortex, early sensory areas process information from the contralateral hemifield, without regard for which effector will ultimately be engaged. In contrast, motor regions are generally organized according to the effector to be moved, without regard for the visuospatial location of the target in space. One might have expected that; as one ascends in the dorsal visual processing stream (Felleman and Van Essen 1991), one would encounter regions with intermediate spatial organization, e.g., a region that responds to visual inputs from either hemifield but lacks specificity for one limb or the other. Such a "pluripotent" reach region would carry signals that represent the intention to reach toward a target, with the limb to be moved determined in a later area. Instead, in PRR, we find an abrupt and complete change—from the visually organized areas from which it receives input (Galletti et al. 2001; Johnson et al. 1996; Passarelli et al. 2011) to a region with properties resembling those of motor areas. Thus the transformation from a general purpose visual signal to an effector-specific intention signal occurs suddenly, within or just before PRR.

This is not to say that PRR behaves similar to the motor cortex in all respects. For example, the reference frame of PRR, although not purely eye centered, is closer to eye centered than to arm centered (Chang and Snyder 2010; McGuire and Sabes 2009). In addition, lesioning PRR strongly affects RT, with weak or no effects on velocity, duration, endpoint scatter, and trajectory. The lesion data indicate that the role of PRR has more to do with registering and conveying the spatial location of a target for a reach rather than controlling the movement itself. Despite this, we have shown that the brain begins making effector-specific motor plans much earlier than has been suggested (Felleman and Van Essen 1991).

One important caveat remains. Our unilateral lesions may have been compensated for by activity in areas outside of the lesion area or by homologous tissue in the other hemisphere. Wilke et al. (2012) show that after a unilateral LIP inactivation, the activity in the contralateral hemisphere is changed. They speculate that this change may reflect a cortical reorganization and go on to suggest that this reorganization may be compensatory for the lesion. It is conceivable that the intact, contralesional PRR is able to compensate for the loss of the lesioned PRR, rescuing the ipsilateral limb from any effects of the lesion. Single-unit activity suggests that reaches with either limb are represented, with a stronger representation for the contralateral limb. Imagine a lesion of the left PRR, abolishing

a strong representation of the right limb and a weaker representation of the left limb. The loss of the weak left limb representation could be masked by the strong representation of the left limb in the intact, right PRR, resulting in no apparent ipsilesional deficit. At the same time, the loss of the strong right limb representation would not be compensated entirely by the intact, weak representation of the right limb, resulting in the contralateral deficit that we see. Indeed, the substrate for such a cross-hemispheric effect exists: PRR has transcallosal connections with itself, as well as with contralateral PMd (Pandya and Vignolo 1969; Seltzer and Pandya 1983). However, the interhemispheric projections from PRR are considerably weaker than those in frontal areas (Seltzer and Pandya 1983). Future studies will use bilateral PRR inactivation to test for the possibility of contralesional compensation.

Our animals were trained to make reaching movements, with or without an accompanying saccade. For simple movements, subjects typically fixate a reach target before the onset of the movement and then maintain fixation until the hand arrives at the target [but see Abrams et al. (1990)]. The onset times of eye and arm movements demonstrate tight temporal coupling (Prablanc et al. 1979; Rogal et al. 1985). It has been suggested that in the monkey, the saccade signals found in PRR may underlie this coupling (Battaglia-Mayer et al. 2001; Boussaoud et al. 1998; Dean et al. 2012; Pesaran et al. 2006). If PRR receives eye-arm coordination signals from an eye-movement area (e.g., LIP), then we would predict that inactivating PRR would impair the use of these signals and thereby, result in weaker temporal coupling, manifest as a decrease in the correlation coefficient between coordinated saccade, and reach RT (Fig. 6*A*). Alternatively, if eye-arm coordination signals flow from PRR to an eye-movement area, then we would predict both impaired correlation, as well as a matched slowing of both saccade and reach RTs (Fig. 6*B*). We observed neither of these outcomes. Instead, reaches were slowed, but saccade timing and eye-arm coordination remained unaffected. This suggests that eye-arm coordination signals flow neither into nor out of PRR and that PRR does not play a major role in coordinating saccade and reach RTs. In a separate study, we have shown that an intervention early in the saccade circuitry (in LIP) slows both coordinated saccades and coordinated reaches but not reaches performed without an accompanying saccade; furthermore, the lesion does not affect eye-arm coordination (Yttri et al. 2013). Taken together, these observations—that neither a LIP nor PRR lesion affects eye-arm coupling, that PRR lesions affect only reach timing, and that LIP lesions affect both saccade and coordinated reaches—suggest (Fig. 8) that eye-arm coordination relies on an active mechanism rather than being driven solely by common inputs; that the cross-coupling occurs later in the reach and saccade pathways than either LIP or PRR; and that the timing of the saccade is used to control the timing of the reach, not vice versa [Jackson et al. 2005; Neggers and Bekkering 1999; but see Horstmann and Hoffmann (2005)].

Relation to studies of human parietal areas. Functional MRI has revealed regions in human parietal cortex (superior parieto-occipital cortex), angular gyrus, and medial IPS that could be homologous to PRR in monkeys. These regions exhibit increased blood oxygen levels when subjects plan reaches or

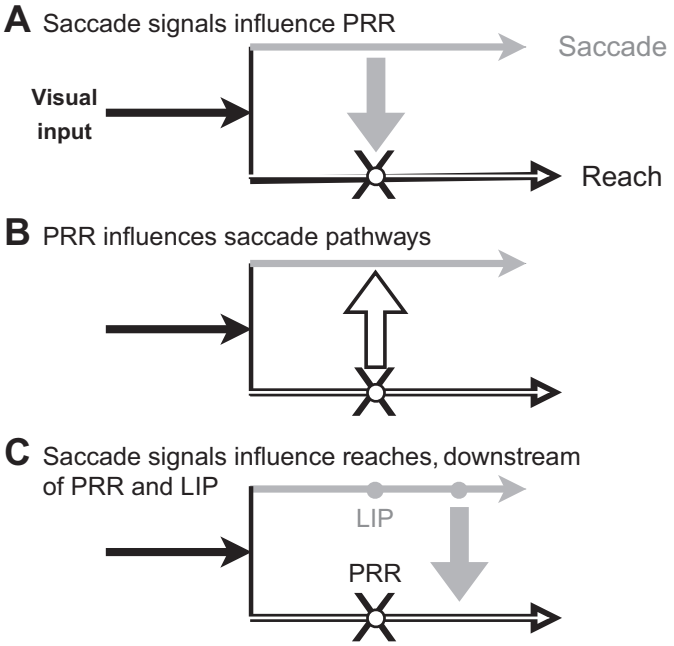

Fig. 8. Schematic indicating possible routes of eye-arm coordination pathway. *A*: a signal from the saccade pathway influences the reach pathway via PRR. *B*: a signal via PRR influences the saccade pathway. *C*: a signal from the saccade pathway downstream of area lateral intraparietal (LIP) influences the reach pathway at a point downstream of PRR. The data favor *C* (see text).

saccades, with greater increases for reaches (Astafiev et al. 2003; Connolly et al. 2003; Fernandez-Ruiz et al. 2007; Grefkes et al. 2004; Hagler et al. 2007; Levy et al. 2007; Medendorp et al. 2003, 2005; Prado et al. 2005). Complementing our findings, Bernier et al. (2012) found changes in blood oxygen level-dependent signals in the dorsomedial posterior parietal cortex in relation to contralateral but not ipsilateral limb reaches. Furthermore, activation was delayed when the subject was required to decide which effector to move, suggesting that effector selection may occur in this area. However, the relationship between parietal regions in monkeys and humans remains unclear. Although in some respects, there are clear parallels, in other respects, the regions differ. For example, human reach regions (medial IPS, angular gyrus) are involved primarily in reaching for targets in the contralateral hemifield (Desmurget et al. 1999; Medendorp et al. 2003, 2005; Vesia et al. 2010). Monkey PRR, in contrast, shows almost no hemifield bias (Fig. 2) (Chang et al. 2008). Interestingly, this pattern (a strong hemifield bias in humans but not in monkeys) is reversed in eye-movement areas: in humans, the parietal eye fields show a comparatively weak hemifield bias [functional MRI (fMRI): Curtis and Connolly (2007); Kagan et al. (2010); Schluppeck et al. (2006)], whereas in monkeys, area LIP is strongly contraversive field specific, independent of the mode of investigation [fMRI: Kagan et al. (2010); Patel et al. (2010); lesions: Liu et al. (2010); Wardak et al. (2002); single-unit recording: Barash et al. (1991)]. Thus there remain substantial cross-species differences in the detailed spatial organization of putatively homologous parietal reach- and saccade-related regions.

Two recent inactivation studies demonstrate that lesions in a region close to PRR affect reaches but not saccades. However, the particulars of these two reports diverge from one another

and in some cases, from the current study (Battaglia-Mayer et al. 2013; Hwang et al. 2012b). First, Hwang et al. (2012b) report hypometria and increased endpoint scatter when reaching to nonfoveal targets. Battaglia-Mayer et al. (2013) report a change in reach trajectory rather than in endpoint. Like Battaglia-Mayer et al. (2013), we found altered reach trajectories but no change in hypometria or endpoint scatter (Table 3 and Fig. 4). Second, Hwang et al. (2012b) report no effect of lesions on either reach or saccade RT. Battaglia-Mayer et al. (2013) find no effects after unilateral injections but see increased saccade and reach RT after bilateral injections. We see increases in reach RT (Table 1). Finally, Battaglia-Mayer and colleagues (2013) report that lesions had no effect on eye-hand correlation, a result that is similar to our findings (Fig. 5). In contrast, a meeting abstract from Hwang et al. (2012a) describes reduced eye-hand correlation.

What accounts for the differences in results across the three studies? One possibility is the use of different injection volumes. Small volumes can lead to a lack of power, whereas large volumes can spread to neighboring (nontargeted) areas. Hwang et al. (2012b) used 4–10 μl/injection. The spread of these injections is not known, since the MR image shown in the publication was made using an unknown injection volume. Battagalia-Mayer et al. (2013) made four separate 1-μl injections. The current study used single 0.5- to 2-μl injections and used MRI to reject injections that spread outside the bounds of PRR.

A second possible reason for different results across studies is that different cortical regions were targeted. Hwang et al. (2012b) and Battagalia-Mayer et al. (2013) targeted *area 5* in the middle portion of the medial bank of the IPS. Hwang et al. (2012b) refer to this anterior region as PRR, although the same lab previously identified *area 5* as anatomically and physiologically distinct from PRR (Buneo et al. 2008). In contrast, the current study targets a more posterior region that reflects earlier definitions of PRR as lying in "the most posterior part of medial bank of the IPS, just anterior to the parietooccipital sulcus" [Scherberger et al. 2003; see also Cui and Andersen (2007); Musallam et al. (2004); Scherberger et al. (2005); all from the same laboratory as Hwang et al. (2012b)]. Nomenclature aside, there are striking differences in the physiology of the anterior area studied by Hwang et al. (2012b) and the posterior region that we injected. The preferred directions of cells in the posterior region are biased, strongly downward, and often contralateral (Chang et al. 2008, 2009; Chang and Snyder 2012). The preferred directions of the more anterior cells recorded in the Hwang et al. (2012b) study (*area 5*) are slightly upward, with an ipsilateral bias in one animal and contralateral bias in the other. This suggests that the anterior and posterior areas are not functionally equivalent, and this may, in turn, explain the discrepant findings after inactivation.

Taken together, these studies argue strongly for a role of the medial IPS in reaching but also reinforce the idea that nearby regions may show very different effects. The technique of imaging actual muscimol injections (Fig. 7) provides a powerful tool to help resolve whether discrepancies across studies are due to different inactivation sites, a spread to regions beyond the intended target, or differences in experimental power.

ACKNOWLEDGMENTS

We thank Jonathon Tucker and Thomas Malone for MRI technical assistance and Matthew Brier for reach trajectory analysis.

GRANTS

Support for this work was provided by National Eye Institute grants EY-012135 and EY-002687, National Institute of Mental Health MH-088522, and National Science Foundation, Integrative Graduate Education and Research Traineeship Program (IGERT), grant 0548890.

DISCLOSURES

The authors have no conflicts of interests.

AUTHOR CONTRIBUTIONS

Author contributions: E.A.Y., Y.L., and L.H.S. conception and design of research; E.A.Y., C.W., and Y.L. performed experiments; E.A.Y., C.W., Y.L., and L.H.S. analyzed data; E.A.Y. interpreted results of experiments; E.A.Y. and C.W. prepared figures; E.A.Y. and L.H.S. drafted manuscript; E.A.Y. and L.H.S. edited and revised manuscript; E.A.Y., C.W., Y.L., and L.H.S. approved final version of manuscript.

REFERENCES

Abrams RA, Meyer DE, Kornblum S. Eye-hand coordination: oculomotor control in rapid aimed limb movements. *J Exp Psychol Hum Percept Perform* 16: 248–267, 1990.

Al-Yahya E, Dawes H, Smith L, Dennis A, Howells K, Cockburn J. Cognitive motor interference while walking: a systematic review and meta-analysis. *Neurosci Biobehav Rev* 35: 715–728, 2011.

Astafiev SV, Shulman GL, Stanley CM, Snyder AZ, Van Essen DC, Corbetta M. Functional organization of human intraparietal and frontal cortex for attending, looking, and pointing. *J Neurosci* 23: 4689–4699, 2003.

Ballard DH, Hayhoe MM, Li F, Whitehead SD. Hand-eye coordination during sequential tasks. *Philos Trans R Soc Lond B Biol Sci* 337: 331–339, 1992.

Barash S, Bracewell RM, Fogassi L, Gnadt JW, Andersen RA. Saccade-related activity in the lateral intraparietal area. II. Spatial properties. *J Neurophysiol* 66: 1109–1124, 1991.

Battaglia-Mayer A, Ferraina S, Genovesio A, Marconi B, Squatrito S, Molinari M, Lacquaniti F, Caminiti R. Eye-hand coordination during reaching. II. An analysis of the relationships between visuomanual signals in parietal cortex and parieto-frontal association projections. *Cereb Cortex* 11: 528–544, 2001.

Battaglia-Mayer A, Ferrari-Toniolo S, Visco-Comandini F, Archambault PS, Saberi-Moghadam S, Caminiti R. Impairment of online control of hand and eye movements in a monkey model of optic ataxia. *Cereb Cortex* 23: 2644–2656, 2013.

Battaglini PP, Muzur A, Galletti C, Skrap M, Brovelli A, Fattori P. Effects of lesions to area V6A in monkeys. *Exp Brain Res* 144, 419–422, 2002.

Battaglini PP, Muzur A, Skrap M. Visuomotor deficits and fast recovery after area V6A lesion in monkeys. *Behav Brain Res* 139: 115–122, 2003.

Bernier PM, Cieslak M, Grafton ST. Effector selection precedes reach planning in the dorsal parietofrontal cortex. *J Neurophysiol* 108: 57–68, 2012.

Biguer B, Jeannerod M, Prablanc C. The coordination of eye, head, and arm movements during reaching at a single visual target. *Exp Brain Res* 46: 301–304, 1982.

Bisley JW, Goldberg ME. Attention, intention and priority in the parietal lobe. *Annu Rev Neurosci* 33: 1–21, 2010.

Boussaoud D, Jouffrais C, Bremmer F. Eye position effects on the neuronal activity of dorsal premotor cortex in the macaque monkey. *J Neurophysiol* 80: 1132–1150, 1998.

Brown JV, Ettlinger G, Garcha HS. Visually guided reaching and tactile discrimination performance in the monkey: the effects of removals of parietal cortex soon after birth. *Brain Res* 267: 67–79, 1983.

Buneo CA, Batista AP, Jarvis MR, Andersen RA. Time-invariant reference frames for parietal reach activity. *Exp Brain Res* 188: 77–89, 2008.

Calton JL, Dickinson AR, Snyder LH. Non-spatial, motor-specific activation in posterior parietal cortex. *Nat Neurosci* 5: 580–588, 2002.

Cavada C. The visual parietal areas in the macaque monkey: current structural knowledge and ignorance. *Neuroimage* 14: S21–S26, 2001.

Chang SW, Dickinson AR, Snyder LH. Limb-specific representation for reaching in the posterior parietal cortex. *J Neurosci* 28: 6128–6140, 2008.

Chang SW, Papadimitriou C, Snyder LH. Using a compound gain field to compute a reach plan. *Neuron* 64: 744–755, 2009.

Chang SW, Snyder LH. Idiosyncratic and systematic aspects of spatial representations in the macaque parietal cortex. *Proc Natl Acad Sci USA* 107: 7951–7956, 2010.

Chang SW, Snyder LH. The representations of reach endpoints in posterior parietal cortex depend on which hand does the reaching. *J Neurophysiol* 107: 2352–2365, 2012.

Cohen YE, Andersen RA. Reaches to sounds encoded in an eye-centered reference frame. *Neuron* 27: 647–652, 2000.

Colby CL, Gattass R, Olson CR, Gross CG. Topographical organization of cortical afferents to extrastriate visual area PO in the macaque: a dual tracer study. *J Comp Neurol* 269: 392–413, 1988.

Connolly JD, Andersen RA, Goodale MA. FMRI evidence for a 'parietal reach region' in the human brain. *Exp Brain Res* 153: 140–145, 2003.

Cui H, Andersen RA. Posterior parietal cortex encodes autonomously selected motor plans. *Neuron* 56: 552–559, 2007.

Curtis CE, Connolly JD. Saccade preparation signals in the human frontal and parietal cortices. *J Neurophysiol* 99: 133–145, 2007.

Dean HL, Hagan MA, Pesaran B. Only coherent spiking in posterior parietal cortex coordinates looking and reaching. *Neuron* 73: 829–841, 2012.

Dean HL, Marti D, Tsui E, Rinzel J, Pesaran B. Reaction time correlations during eye-hand coordination: behavior and modeling. *J Neurosci* 31: 2399–2412, 2011.

Desmurget M, Epstein CM, Turner RS, Prablanc C, Alexander GE, Grafton ST. Role of the posterior parietal cortex in updating reaching movements to a visual target. *Nat Neurosci* 2: 563–567, 1999.

Felleman DJ, Van Essen DC. Distributed hierarchical processing in the primate cerebral cortex. *Cereb Cortex* 1: 1–47, 1991.

Fernandez-Ruiz J, Goltz HC, DeSouza JF, Vilis T, Crawford JD. Human parietal "reach region" primarily encodes intrinsic visual direction, not extrinsic movement direction, in a visual motor dissociation task. *Cereb Cortex* 17: 2283–2292, 2007.

Fischer B, Rogal L. Eye-hand-coordination in man: a reaction time study. *Biol Cybern* 55: 253–261, 1986.

Fisk JD, Goodale MA. The organization of eye and limb movements during unrestricted reaching to targets in contralateral and ipsilateral visual space. *Exp Brain Res* 60: 159–178, 1985.

Galletti C, Fattori P, Gamberini M, Kutz DF. The cortical visual area V6: brain location and visual topography. *Eur J Neurosci* 11: 3922–3936, 1999.

Galletti C, Gamberini M, Kutz DF, Fattori P, Luppino G, Matelli M. The cortical connections of area V6: an occipito-parietal network processing visual information. *Eur J Neurosci* 13: 1572–1588, 2001.

Gamberini M, Passarelli L, Fattori P, Zucchelli M, Bakola S, Luppino G, Galletti C. Cortical connections of the visuomotor parietooccipital area V6Ad of the macaque monkey. *J Comp Neurol* 513: 622–642, 2009.

Gottlieb JP, Kusunoki M, Goldberg ME. The representation of visual salience in monkey parietal cortex. *Nature* 391: 481–484, 1998.

Grefkes C, Ritzl A, Zilles K, Fink GR. Human medial intraparietal cortex subserves visuomotor coordinate transformation. *Neuroimage* 23: 1494–1506, 2004.

Hagler DJ, Riecke L, Sereno MI. Parietal and superior frontal visuospatial maps activated by pointing and saccades. *Neuroimage* 35: 1562–1577, 2007.

Horstmann A, Hoffmann KP. Target selection in eye-hand coordination: do we reach to where we look or do we look to where we reach? *Exp Brain Res* 167: 187–195, 2005.

Hwang E, Hauschild M, Wilke M, Andersen R. Causal evidence for the parietal reach region involvement in eye-hand coordination during free-gaze (Abstract). *Soc Neurosci* 2012a.

Hwang EJ, Hauschild M, Wilke M, Andersen RA. Inactivation of the parietal reach region causes optic ataxia, impairing reaches but not saccades. *Neuron* 76: 1021–1029, 2012b.

Jackson SR, Newport R, Mort D, Husain M. Where the eye looks, the hand follows; limb-dependent magnetic misreaching in optic ataxia. *Curr Biol* 15: 42–46, 2005.

Johnson PB, Ferraina S, Bianchi L, Caminiti R. Cortical networks for visual reaching: physiological and anatomical organization of frontal and parietal lobe arm regions. *Cereb Cortex* 6: 102–119, 1996.

Kagan I, Iyer A, Lindner A, Andersen RA. Space representation for eye movements is more contralateral in monkeys than in humans. *Proc Natl Acad Sci USA* 107: 7933–7938, 2010.

Kutz DF, Fattori P, Gamberini M, Breveglieri R, Galletti C. Early- and late-responding cells to saccadic eye movements in the cortical area V6A of macaque monkey. *Exp Brain Res* 149: 83–95, 2003.

Lamotte RH, Acuña C. Defects in accuracy of reaching after removal of posterior parietal cortex in monkeys. *Brain Res* 139: 309–326, 1978.

Levy I, Schluppeck D, Heeger DJ, Glimcher PW. Specificity of human cortical areas for reaches and saccades. *J Neurosci* 27: 4687–4696, 2007.

Liu Y, Yttri EA, Snyder LH. Intention and attention: different functional roles for LIPd and LIPv. *Nat Neurosci* 13: 495–500, 2010.

Luppino G, Ben Hamed S, Gamberini M, Matelli M, Galletti C. Occipital (V6) and parietal (V6A) areas in the anterior wall of the parieto-occipital sulcus of the macaque: a cytoarchitectonic study. *Eur J Neurosci* 21: 3056–3076, 2005.

McGuire LM, Sabes PN. Sensory transformations and the use of multiple reference frames for reach planning. *Nat Neurosci* 12: 1056–1061, 2009.

Medendorp WP, Goltz HC, Crawford JD, Vilis T. Integration of target and effector information in human posterior parietal cortex for the planning of action. *J Neurophysiol* 93: 954–962, 2005.

Medendorp WP, Goltz HC, Vilis T, Crawford JD. Gaze-centered updating of visual space in human parietal cortex. *J Neurosci* 23: 6209–6214, 2003.

Milnik A, Nowak I, Müller NG. Attention-dependent modulation of neural activity in primary sensorimotor cortex. *Brain Behav* 3: 54–66, 2013.

Musallam S, Corneil BD, Greger B, Scherberger H, Andersen RA. Cognitive control signals for neural prosthetics. *Science* 305: 258–262, 2004.

Neggers SF, Bekkering H. Integration of visual and somatosensory target information in goal-directed eye and arm movements. *Exp Brain Res* 125: 97–107, 1999.

Pandya DN, Seltzer B. Intrinsic connections and architectonics of posterior parietal cortex in the rhesus monkey. *J Comp Neurol* 204: 196–210, 1982.

Pandya DN, Vignolo L. Interhemispheric projections of the parietal lobe in the rhesus monkey. *Brain Res* 15: 49–65, 1969.

Passarelli L, Rosa MG, Gamberini M, Bakola S, Burman KJ, Fattori P, Galletti C. Crtical connections of area V6Av in the macaque: a visual-input node to the eye/hand coordination system. *J Neurosci* 31: 1790–1801, 2011.

Patel GH, Shulman GL, Baker JT, Akbudak E, Snyder AZ, Snyder LH, Corbetta M. Topographic organization of macaque area LIP. *Proc Natl Acad Sci USA* 107: 4728–4733, 2010.

Pesaran B, Nelson MJ, Andersen RA. Dorsal premotor neurons encode the relative position of the hand, eye, and goal during reach planning. *Neuron* 51: 125–134, 2006.

Prablanc C, Echallier JF, Komilis Jeannerod ME. Optimal response of eye and hand motor systems in pointing at a visual target. I. Spatio-temporal characteristics of eye and hand movements and their relationships when varying the amount of visual information. *Biol Cybern* 35: 113–124, 1979.

Prado J, Clavagnier S, Otzenberger H, Scheiber C, Kennedy H, Perenin MT. Two cortical systems for reaching in central and peripheral vision. *Neuron* 48: 849–858, 2005.

Quian Quiroga R, Snyder LH, Batista AP, Cui H, Andersen RA. Movement intention is better predicted than attention in the posterior parietal cortex. *J Neurosci* 26: 3615–3620, 2006.

Rogal L, Reible G, Fischer B. Reaction times of the eye and the hand of the monkey in a visual reach task. *Neurosci Lett* 58: 127–132, 1985.

Rushworth MF, Nixon PD, Passingham RE. Parietal cortex and movement. I. Movement selection and reaching. *Exp Brain Res* 117: 292–310, 1997.

Scherberger H, Fineman I, Musallam S, Dubowitz DJ, Bernheim KA, Pesaran B, Corneil BD, Gilliken B, Andersen RA. Magnetic resonance image-guided implantation of chronic recording electrodes in the macaque intraparietal sulcus. *J Neurosci Methods* 130: 1–8, 2003.

Scherberger H, Jarvis MR, Andersen RA. Cortical local field potential encodes movement intentions in the posterior parietal cortex. *Neuron* 46: 347–354, 2005.

Schluppeck D, Curtis CE, Glimcher PW, Heeger DJ. Sustained activity in topographic areas of human posterior parietal cortex during memory-guided saccades. *J Neurosci* 26: 5098–5108, 2006.

Seltzer B, Pandya DN. The distribution of posterior parietal fibers in the corpus callosum of the rhesus monkey. *Exp Brain Res* 49: 147–150, 1983.

Snyder LH, Batista AP, Andersen RA. Coding of intention in the posterior parietal cortex. *Nature* 386: 167–170, 1997.

Snyder LH, Batista AP, Andersen RA. Saccade-related activity in the parietal reach region. *J Neurophysiol* 83: 1099–1102, 2000.

Snyder LH, Dickinson AR, Calton JL. Preparatory delay activity in the monkey parietal reach region predicts reach reaction times. *J Neurosci* 26: 10091–10099, 2006.

Vesia M, Prime SL, Yan X, Sergio LE, Crawford JD. Specificity of human parietal saccade and reach regions during transcranial magnetic stimulation. *J Neurosci* 30: 13053–13065, 2010.

Wardak C, Olivier E, Duhamel JR. A deficit in covert attention after parietal cortex inactivation in the monkey. *Neuron* 42: 501–508, 2004.

Wardak C, Olivier E, Duhamel JR. Saccadic target selection deficits after lateral intraparietal area inactivation in monkeys. *J Neurosci* 22: 9877–9884, 2002.

Wilke M, Kagan I, Andersen RA. Functional imaging reveals rapid reorganization of cortical activity after parietal inactivation in monkeys. *Proc Natl Acad Sci USA* 109: 8274–8279, 2012.

Yttri EA, Liu Y, Snyder LH. Lesions of LIP affect reach onset only when the reach is accompanied by a saccade, revealing an active eye-hand coordination circuit. *Proc Natl Acad Sci USA* 110: 2371–2376, 2013.